

Article

# Spatial Distribution of Stony Desertification and Key Influencing Factors in Different Sampling Scales in Small Karst Watersheds

Zhenming Zhang<sup>1,2</sup>, Yunchao Zhou<sup>1,2,3\*</sup>, Shijie Wang<sup>3,4</sup>, Xianfei Huang<sup>1,2</sup>

<sup>1</sup> Forest Resource and Environment Research Center of Guizhou Province, Guizhou University, Guiyang 550025, China; zhang6653579@163.com (Z.Z.); huangxianfei1983@163.com (X.H.)

<sup>2</sup> College of Forestry, Guizhou University, Guiyang 550025, China

<sup>3</sup> Puding Karst Ecosystem Research Station of Guizhou Province, Puding 562100, China; zhang6653578@163.com (S.W.)

<sup>4</sup> State Key Laboratory of Environmental Geochemistry, Institute of Geochemistry, Chinese Academy of Science, Guiyang 550002, China

\* Correspondence: yczhou@gzu.edu.cn; Tel.: +86-151-8519-6301

**Abstract:** In this paper, the spatial distribution of stony desertification characteristics and its influencing factors in Karst areas in different sampling scales are studied using a grid sampling method based on geographic information system (GIS) technology and geo-statistics, with the rock bareness rate obtained through sampling with 150m × 150m grids in the Houzhai River Basin being taken as the original data and five grid scales (300m × 300m, 450m × 450m, 600m × 600m, 750m × 750m, and 900m × 900m) as the subsample sets. The results show that the rock bareness rate does not vary much from one sampling scale to another while average values of the five sub-samples all fluctuate around the average value of the entire set. As the sampling scale is expanding, the maximum value and the average value of rock bareness rate are decreasing gradually, with a gradual increase in the coefficient of variability. In the scale of 150m × 150m, the areas of minor stony desertification, medium stony desertification, and major stony desertification in the Houzhai River Basin are 7.81 km<sup>2</sup>, 4.50 km<sup>2</sup>, and 1.87 km<sup>2</sup>, respectively. The spatial variability of stony desertification on small scales is influenced by many factors, and that on medium scales is jointly influenced by gradient, rock contents, and rock bareness rate. On large scales, the spatial variability of stony desertification is mainly influenced by soil thickness and rock bareness rate.

**Keywords:** different sampling scales; spatial distribution; stony desertification characteristics; Karst; small watershed

## 1. Introduction

Soil is continuum with uneven changes, and the soil property value presents obvious spatial variability [1]. The research foundation of soil science is to obtain detailed and accurate spatial distribution information of soil property [2]. The sampling scale has decisive influences on acquisition accuracy and quantitative expression of soil property and spatial variability information [3].

Theoretically, the narrower the sampling scale, the less the interpolation prediction error. If sampling is oversized, it is difficult to guarantee the interpolation accuracy [4]. However, excessively high sampling density will cause more consumption of manpower, material resources and financial resources and long work cycle [5]. How to determine a reasonable sampling density during regional research on soil science is a key and difficult point of present research on soil science [6]. Different sampling scales lead to different characteristics, including different influencing factors and different evolution mechanisms and processes [7]. Therefore, only if the sampling scale is in line with the intrinsic scale of the phenomenon to be studied can the key influencing factors be revealed reliably. In Karst areas, the earth's surface is uneven greatly, the landscape is broken extremely, and the key influencing factors vary with sampling scales.

The concept of stony desertification was first proposed in the early 1980s, and later, it was defined as a term representing the process of the transition from vegetation-covered and soil-covered Karst areas to Karst landscapes covered by bare rocks [8]. Karst areas in China are typical areas ecologically fragile, the stony desertification problem of which has become the most serious ecological and economic problem as well as the source of disasters and poverty there [9]. According to the experience on treating typical stony desertification areas, the treatment requires guidance of driving mechanisms and theories on different spatial scales [10]. In particular, it is necessary to determine positive and negative impacts of natural and human effects on the progress of stony desertification as well as their respective contribution rates [11]. Therefore, distribution characteristics of stony desertification and their relations with environmental factors on different sampling scales are of great importance for understanding of the progress of Karst ecosystem and have received wide attention [12]. At present, majority of studies on spatial distribution of stony desertification are limited to single factors and about the spatial correlation [13-14]. There are very rare comprehensive and systematic quantitative analyses of impacts of various factors on spatial distribution of stony desertification, even fewer studies on problems about differences in scale. In this paper, GIS and geo-statistics are combined together to reveal studies on spatial distribution characteristics of stony desertification in different sampling scales. Multiple stepwise regression and Pearson correlation analysis are used to explore the key influencing factors of stony desertification characteristics on non-sampling scales and aimed at revealing determinants of the spatial distribution of stony desertification and the differences among different scales, providing references for treatment of stony desertification in Karst areas.

## 2. Materials and Methods

### 2.1. Study Area

The study region (105°40'43"-105°48'2"E, 26°12'29"-26°17'15"N) is located in Puding County in the central part of Guizhou Province in southwestern China, including the three towns of Chengguan (CG), Maguan (MG) and Baiyan (BY), and it covers an area of 72 km<sup>2</sup>. The elevation is between 1223.4 and 1567.4 m above sea level, and the air pressure is between 806.1 and 883.8 hpa. There are three major categories of soil: limestone soil, paddy soil and yellow soil. The vegetation (Table 1) includes cedarwood (*Cupressus funebris* Endl.), populus adenopoda (*Populus Adenopoda* Maxim), toona sinensis (*Toona sinensis* (A. Juss.) Roem.), Chinese pear (*Pyrus pyrifolia* Burm Nakai.), and so on. The main crops are paddy rice (*Oryzasativa Oryzaglaberrima*), corn (*Zea mays* Linn. Sp.), soybean (*Glycine max* (Linn.) Merr), sunflower (*Helianthus annuus*), etc. There are 7 soil types in the study area: Xan Udic Fernalisols, Black Lithomorphic Isohumisols, Cab Udi Orthic Entisols, Cab High

fertility Orthic Anthrosol, Cab Low fertility Orthic Anthrosols, Cab Medium fertility Orthic Anthrosols, Fec Hydragric Anthrosols.

## 2.2 Data Source

Sampling plots were designed with a grid-based sampling method and a total of 2755 sampling grids (150 m×150 m), consisting of 22057 soil samples, The sampling depth is 20cm. The sampling sites were defined as the center of each sampling grid (Figure 1). The soil samples were air dried, ground and prepared for the specimen as required by the laboratory; then, the SOC content was tested and analyzed. The SOC was determined via a potassium dichromate method.

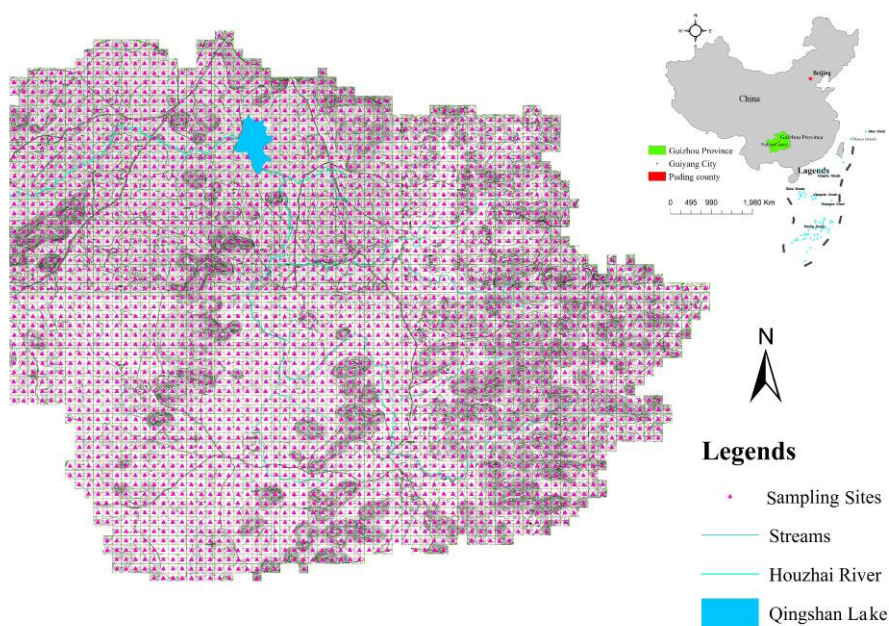


**Figure 1.** The location of Houzhai River basin and the distribution of sample sites.

## 2.3 Classification of Different Grid Scales

The grid scale determines the density and data of sampling point. To study the impacts of different sampling scales on the revelation of spatial variability of soil organic carbon, ArcGIS software is adopted to amplify the 2,755 grids of 150m×150m by one time to get 802 grids of 300m×300m, and then classify these grids into six grid scales: 450m×450m, 600m×600m, 750m×750m and 900m×900m (Figure 2). Meanwhile, to ensure the reliability of the conclusions and reduce the unreliability resulted from repeated sampling, subsets of five samples are drawn with unrepeated sampling methods.

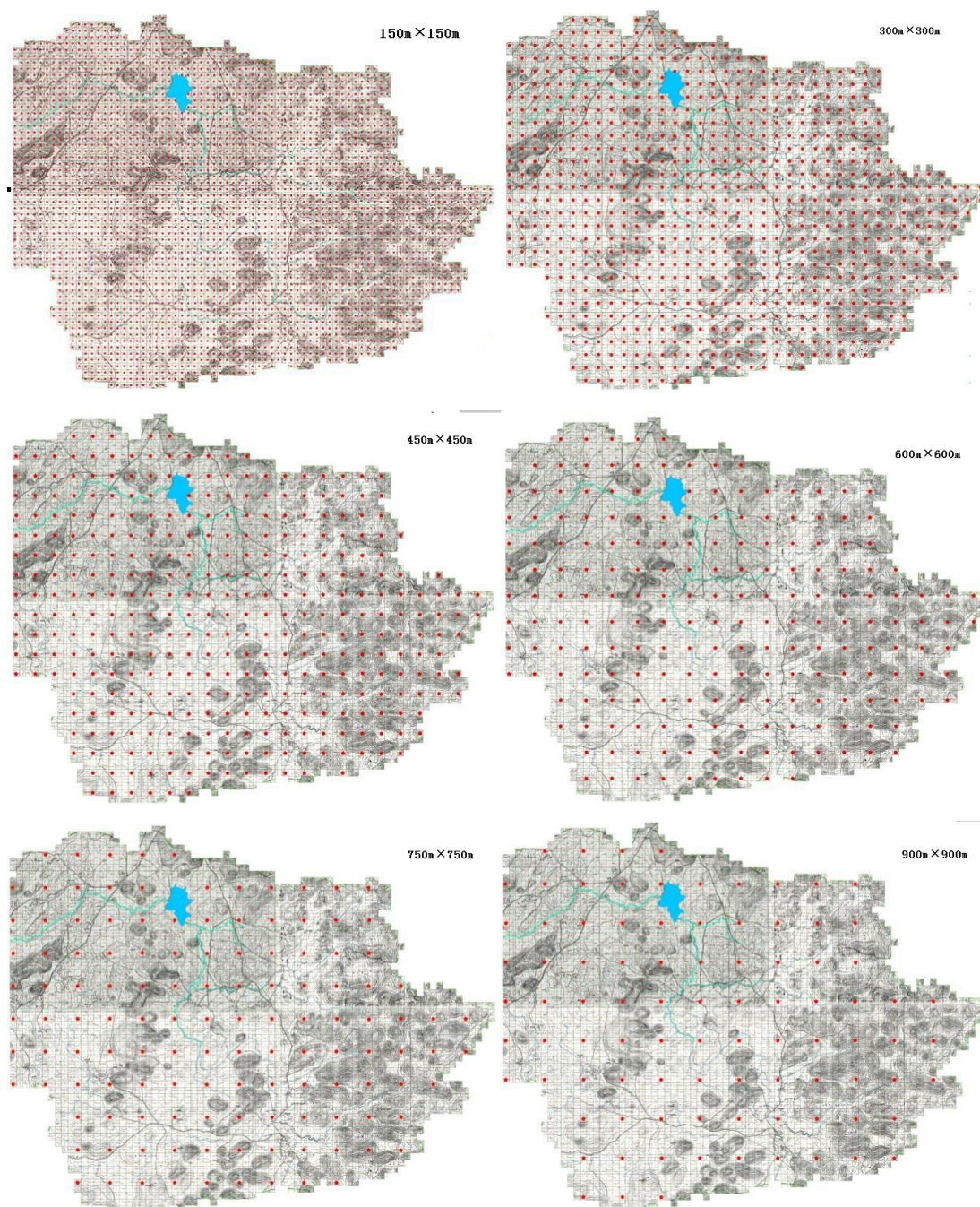


**Figure 2.** Plots of soil sample distribution under different sampling scales.

#### 2.4 Calculations and Statistical Analysis

A semi-variance function ( $h$ ) was used to describe the spatial heterogeneity of the soil properties. The semi variance function was used to obtain the variation of the semi-variance function value with an increase in the distance of the sample; the scatter plots were fitted with a Gaussian model and other theoretical models. When the soil properties met a two-order stationary assumption and the intrinsic hypothesis and when the sample size was large enough, the semi-variance theory variation function ( $h$ ) formula was used. The semivariance ( $r(h)$ ) is as follows [15]:

$$r(h) = \frac{1}{2N(h)} \sum_{i=1}^{N(h)} [Z(x_i) - Z(x_i+h)]^2 \quad (1)$$

Where  $Z$  is the measured soil property,  $x$  is the sample location, and  $N(h)$  is the number of pairs of locations separated by a lag distance  $h$ . The semivariogram expresses the relationship between the semivariance and the lag distance ( $h$ ). It typically increases from a value at  $h = 0$  (identified as the nugget) to a maximum value (identified as the sill). The SOCD of the spatial distribution pattern was determined using a kriging interpolation method with a spatial interpolation grid.

Statistical analysis was performed using SPSS18.0 and Excel2007. A semi-variogram model, fitted with GS+ software, was used for ordinary kriging interpolation in ArcGIS 9.3 software, rendering an organic carbon density spatial distribution map.

### 3. Results and Analysis

#### 3.1 Descriptive statistics for coverage of rock exposures at different sampling scales

Table 1 provides the statistics on the coverage of rock exposures (CRE) at different sampling scales. The statistics reveal a wide gap between the maximum and minimum CRE in the Houzhai River basin, which are 95.00% and 0.00, respectively. The CRE varied slightly with the sampling scale. The 150 m  $\times$  150 m sample has the highest average CRE, at 15.94%, while the 900 m  $\times$  900 m sample shows the lowest average CRE, at 9.89%. The former is 1.62 times the latter. As the sampling scale increases, the maximum and average values of CRE gradually decrease while the coefficient of variation increases.

Coefficient of variation (CV) is a measure of dispersion of distribution of a random variable, i.e. the extent of spatial variability in an attribute indicator. Normally CV values no greater than 10% indicate low variability, CV values between 10% and 100% indicate moderate variability, and CV values greater than 100% signify high variability. The CV in CRE across the Houzhai River basin ranges from 139.84% to 197.67% (Table 1), suggesting high CRE variability at various sampling scales. It follows that the coverage of rock exposures significantly varies spatially within the study area. The average CRE values for the five subsamples fluctuate around the average CRE for each sample set, indicating that the subsamples have consistent statistical characteristics with the sample and thus are representative, despite the small number of sampling points in each sample. The CV in CRE first increases and then decreases with increasing sampling scale. Moreover, the CRE is normally distributed in the sample sets and all subsamples in terms of both skewness and kurtosis.

**Table 1.** Description and statistics of rock exposures under different sampling scales.

Sampling scales	Sample size	Minimum	Maximum	Mean	Standard deviation	Coefficient of variation	skewness	Kurtosis
150m $\times$ 150m	2755	0.00	95.00	15.94	22.29	139.84	1.33	0.79
300m $\times$ 300m	802	0.00	92.00	12.89	21.42	166.18	1.90	1.69
450m $\times$ 450m	357	0.00	88.00	12.18	20.71	170.03	1.35	0.78
600m $\times$ 600m	200	0.00	85.00	11.97	20.51	171.35	1.99	1.71
750m $\times$ 750m	128	0.00	75.00	10.22	17.52	171.43	2.29	1.72
900m $\times$ 900 m	91	0.00	73.00	9.89	19.55	197.67	2.52	1.83

#### 3.2 Semivariograms describing coverage of rock exposures at different sampling scales

Classical statistical methods can be used to describe some overall characteristics of CRE, but they are unable to characterize its spatial variability. Therefore, this study used a geostatistical method to quantify the constitutive properties and randomness of CRE in order to analyze the pattern of spatial variation in CRE more accurately. The CRE data obtained at different sampling scales were fitted with semivariograms using the software GS+7.0 (Table 2). As can be seen in Table 2, the CRE values across the study area follow an exponential distribution at different sampling scales. Use the 150m×150m sample set as the reference and then compare the semivariograms for the five sample subsets against the semivariogram for the sample set. It was found that the codomain of CRE decreases steadily with increasing sampling set. This is possible because a larger sampling scale is associated with the smaller number of samples and thus lower levels of uniformity in the indicators considered. Nugget effect ( $C_0$ ) is usually used to measure the variation due to experimental error and negative deviation from actual sampling scale, i.e. spatial heterogeneity caused by random factors. Table 2 shows that  $C_0$  peaks in the 150m×150m sample set and declines with increasing sampling scale. This means that the amount of variation caused by random factors tends to decrease as the sample scale increases, possibly because a decrease in sampling scale will increase the number of random factors involved and the complexity of causes of variability, and thus more secondary causes will be neglected.

The Nugget coefficient of semivariogram, defined as  $C_0/C_0+C$ , is 0.512 for the 150m×150m sample set and 0.500 for the 300m×300m sample set. The Nugget coefficient is smaller than 0.5 at the scale of 450m×450m, and it begins to decrease as sampling scale further increases. This suggests strong spatial dependence of CRE at sampling scales greater than 450m×450m. This is possible because the spatial dependence caused by structural and random factors at small scales is covered by that at larger scales. Therefore, an increase in sampling scale can strengthen the effects of structural factors and thereby lead to variability in spatial variability within a certain region.

**Table 2.** Semi variance model of rock exposures and its fitting parameters under different sampling scales.

Sampling scales	Model type	Nugget ( $C_0$ )	Sill ( $C_0+C$ )	Range /m	$C_0/C_0+C$	$R^2$	RMSE
150m×150m	Index	0.088	0.172	2960	0.512	0.848	0.673
300m×300m	Index	0.076	0.152	2350	0.500	0.831	0.612
450m×450m	Index	0.068	0.272	2630	0.250	0.772	0.478
600m×600m	Index	0.062	0.243	2140	0.255	0.636	0.281
750m×750m	Index	0.043	0.196	1970	0.219	0.779	0.222
900m×900m	Index	0.041	0.187	1860	0.219	0.782	0.228

### 3.3 Spatial characteristics of rocky desertification in a small catchment area in karst

Based on the spatial characteristics of coverage of bedrock exposures in the Houzhai River basin and methods of rocky desertification classification provided by previous research, this study classifies the extent of rocky desertification in this area into the following grades: (1) non-karst region unaffected by rocky desertification: coverage of bedrock exposures < 20%; (2) potential rocky desertification: 20% ≤ coverage of bedrock exposures < 30%; (3) slight rocky desertification: 30% ≤ coverage of bedrock exposures < 50%; (4) moderate rocky desertification: 50% ≤

coverage of bedrock exposures  $< 70\%$ ; (5) severe rocky desertification:  $70\% \leq$  coverage of bedrock exposures  $< 90\%$ . The data from the present study shows that at the scale of  $150\text{m} \times 150\text{m}$ , the slight, moderate, and severe rocky desertification covers an area of  $7.81 \text{ km}^2$ ,  $4.50 \text{ km}^2$ , and  $1.87 \text{ km}^2$ , respectively, in the Houzhai River basin.

Rocky desertification in the study area is distributed primarily in the peak-cluster depressions from the northwest to the southeast. As the sampling scale increases, the distribution of severe rocky desertification varies significantly in the southeastern region, while the distribution of moderate rocky desertification varies little (shown in Figure2). The northern and central parts of the study area exhibit extensive shrinkage of rocky desertification, while the coverage of rocky desertification decreases sporadically in the northern part. The expansion of severe rocky desertification is concentrated in the Yuyangzhai and Dayouzhai villages in the southeast and the Chenqi, Houshan, and Zhaojiatian villages in the north. The trend in the extent of rocky desertification with the number of samples can better characterize the actual evolution of rocky desertification. All the variations in the rocky desertification of different grades found in the study area are driven by a combination of natural and human factors. The factors affecting rocky desertification vary with sampling scales. Therefore, finding out the different driving factors behind the variations can facilitate more reasonable sampling in research on rocky desertification.

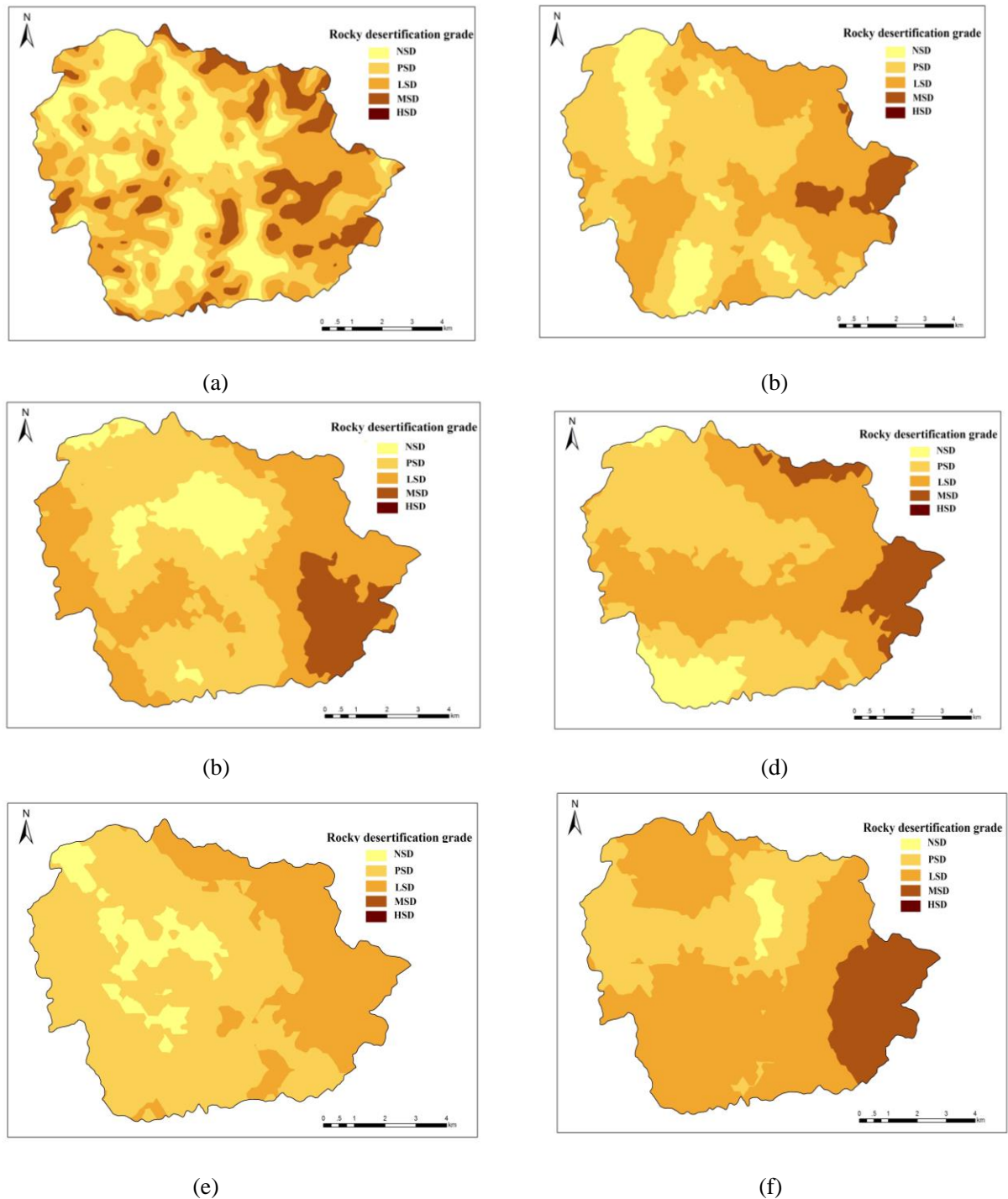


**Figure 2.** Spatial distribution map of rocky desertification under different sampling scales:

(a) is sampling scale of 150 m×150m; (b) is sampling scale of 300 m×300m; (c) is sampling scale of 450 m×450m; (d) is sampling scale of 600 m×600m; (e) is sampling scale of 750 m×750m; (f) is sampling scale of 900 m×900m. NSD is non-karst region; PSD is potential rocky desertification; LSD is slight rocky desertification; MSD is moderate rocky desertification; HSD is severe rocky desertification.

### 3.4 Factors affecting the characteristics of rocky desertification at different sampling scales

As the grade of rocky desertification depends on CRE, this study uses factors affecting CRE to



characterize factors affecting rocky desertification (Table 4). A Pearson correlation analysis shows that at the scale of 150m×150m, the CRE has extremely significant and positive correlations with slope and elevation ( $P < 0.01$ ), and the correlation coefficients are 0.893 and 0.991, respectively. It has an extremely significant and negative correlation with soil thickness ( $P < 0.01$ ), with the correlation coefficient being -0.910. A significant positive correlation exists between the CRE and slope position ( $P < 0.05$ ), with the correlation coefficient being 0.480. The correlations between the CRE and soil bulk density and rock content were not significant ( $P > 0.05$ ). At the scale of 300m×300m, the CRE has a significant negative correlation with soil thickness ( $r = -0.732$ ) ( $P < 0.05$ ), significant positive correlations elevation ( $r = 0.512$ ) and rock content ( $r = 0.610$ ) ( $P < 0.05$ ). Its correlations with slope ( $r = 0.721$ ) and slope position ( $r = 0.913$ ) are extremely significant and positive ( $P < 0.01$ ). There is no obvious correlation between CRE and soil bulk density. At the scale of 450m×450m, the CRE has extremely significant and positive correlations with slope, elevation, rock content, and slope position ( $P < 0.01$ ,  $r = 0.763, 0.813, 0.913, \text{ and } 0.680$ , respectively). At the scale of 600m×600m, the CRE shows an extremely significant and positive correlation with rock content ( $P < 0.01$ ,  $r = 0.684$ ). It has significant, positive correlations with slope and slope position ( $P < 0.05$ ), with the correlation coefficients being 0.503 and 0.406. There is no significant correlation between the CRE and other factors. At the scale of 750m×750m, the CRE is positively and significantly correlated with rock content and slope position ( $P < 0.05$ ), with correlation coefficients of 0.780 and 0.741, respectively. At the scale of 900m×900m, the CRE has an extremely significant and negative correlation with soil thickness ( $P < 0.01$ ,  $r = -0.632$ ) and a strong positive correlation with slope position ( $P < 0.05$ ), with the correlation coefficient being 0.501.

**Table 4.** Correlation matrix of rock exposures and its influencing factors under different sampling scales.

Sampling scale	Slope	Altitude	Soil thickness	Soil bulk density	rock content	slope position
150m×150m	0.893**	0.991**	-0.910**	-0.832	0.510	0.480*
300m×300m	0.721**	0.512*	-0.732*	-0.632	0.610*	0.913**
450m×450m	0.763**	0.813**	0.456	0.612	0.913**	0.680**
600m×600m	0.503*	0.453	0.736	0.486	0.684**	0.406*
750m×750m	0.421	0.112	0.432	0.362	0.780*	0.741*
900m×900m	0.689	0.363	-0.632**	0.462	0.496	0.501*

\*\* indicates that the correlation is significant when the confidence level (double measure) is 0.01.

\* the correlation is significant when the confidence level (double measure) is 0.05.

Regression equations fitted to the CRE data are shown in Table 5. The values of coefficient of determination ( $R^2$ ) reveal that distribution of soil bulk density has the poorest fit at all sampling scales, which indicates a relatively weak correlation between soil bulk density and CRE. As the scale increases, the distributions of topographic factors (elevation and slope) and rock content improve in goodness of fit to CRE. Overall, an increase in the sampling scale can improve the goodness of fit of the equations. The data obtained at a large scale (e.g. 900m×900m) can describe the relationships between CRE and the factors more accurately, while the data acquired at a small scale (e.g. 150m×150m) can be less able to reflect their relationships due to the influence of complex microtopography. Therefore, decreasing the sampling scale may decrease the goodness of fit between CRE and various influencing factors.

It is clear from the aforementioned findings that the key driving factors behind the spatial

variability in CRE differ depending on the sampling scale. At small scales (150m×150m, 300m×300m and 450m×450m), the spatial variations in CRE are affected by a combination of slope, elevation, soil thickness, and CRE. At a medium scale (600m×600m), the spatial variations in CRE depend on slope, rock content, and CRE. At large scales (750m×750m and 900m×900m), soil thickness and CRE are the key factors influencing the variability in CRE. As the sampling scale increases, the structural features attributed to the concentration of multiple complex factors over short distances are hidden by the factors that affect CRE over longer distances, such as soil thickness and CRE. This explains why the topographic factors that have relatively stable and continuous distributions (soil thickness and CRE) show stronger correlations with CRE at large scales.

**Table 5.** Optimal fitting equation of influence factors and rock exposures under different sampling scales.

Sampling scale	Index	The optimal fitted equation for rock exposures	R <sup>2</sup>
150m×150m	Slope	$y=0.0112x+12.539$	0.263
	Altitude	$y=0.166x +1288.201$	0.287
	Soil thickness	$y=0.0212x+11.592$	0.272
	Soil bulk density	$y=-0.0255\ln(x)+1.1502$	0.011
	slope position	$y=0.1x^2+0.031x +9.358$	0.382
	rock content	$y=1.3256\ln(x)-1.4693$	0.369
300m×300m	Slope	$y=0.0194x+22.384$	0.343
	Altitude	$y=0.0194x+1425.084$	0.298
	Soil thickness	$y=0.0194x+15.084$	0.349
	Soil bulk density	$y=1.2081\ln(x)+11.31$	0.017
	slope position	$y=0.2x^2+0.0048x+5.695$	0.439
	rock content	$y=1.2682\ln(x)-12.225$	0.428
450m×450m	Slope	$y=0.0231x+10.148$	0.391
	Altitude	$y=-2.3608x+1314.8$	0.317
	Soil thickness	$y=-0.0216x+17.978$	0.361
	Soil bulk density	$y=1.3498\ln(x)+12.466$	0.018
	slope position	$y=0.2x^2-0.1014x+0.2054$	0.463
	rock content	$y = -3.2414\ln(x) + 21.321$	0.474

600m×600m	Slope	$y=0.0182x+24.713$	0.412
	Altitude	$y = 0.430e^{0.013x}$	0.331
	Soil thickness	$y = 43.525 - 0.950x + 0.105x^2$	0.372
	Soil bulk density	$y = 1.2014\ln(x) + 13.823$	0.020
	slope position	$y = 0.0003x^2 + 0.0681x + 15.567$	0.514
	rock content	$y = 1.0924\ln(x) + 21.854$	0.548
750m×750m	Slope	$y = 0.1313x + 23.153$	0.497
	Altitude	$y = 0.101x + 1033.201$	0.395
	Soil thickness	$y = -0.1625x + 65.293$	0.619
	Soil bulk density	$y = 3.1781\ln(x) + 15.597$	0.022
	slope position	$y = 0.002x^2 - 0.0855x + 16.946$	0.587
	rock content	$y = 0.1313x + 22.053$	0.649
900m×900m	Slope	$y = 0.2669x - 0.0397$	0.516
	Altitude	$y = 0.136x + 1083.201$	0.491
	Soil thickness	$y = 0.1325x + 24.78$	0.673
	Soil bulk density	$y = 0.9136\ln(x) + 21.2$	0.029
	slope position	$y = 0.0023x^2 - 0.1766x + 17.997$	0.645
	rock content	$y = 0.8333\ln(x) + 21.429$	0.703

## 4 Discussion

### 4.1 Relations between Sampling Scales and Stony Desertification

In general, there are two kinds of understandings about study scales: one is to conduct multi-scale studies within a fixed study area by encrypting or broadening number of samples, and the other is to conduct multi-scale studies by changing the study areas from small ones to large ones. The two reveal different factors or processes and have different characteristics [16]. In many studies on multi-scale effects of soil attributes, majority of people choose the second method, that is, to conduct multi-scale studies by expanding the study area, put more emphasis on the deduction of studies on different scales, and reveal the multi-scale spatial changing relations after expansion of study areas from small ones to large ones, which can better illustrate multi-scale effects of the study areas on the macro level [17]. However, inevitably this study method cannot meet the demands of multi-scale studies using fixed areas to reflect the global scope, which leads to the problem that within the entire study area, a scale can only reflect local soil characteristic information within the sampling range, unable to globally describe soil characteristics on different sampling scales [18]. However, it is inevitable that changes to

scales will lead to fluctuations of variability, resulting in deviations between apparent variations and real variations [19]. In particular, the Karst areas cannot reflect the influencing factors of stony desertification areas very well [20]. In view of this, in this study, small watersheds are taken as the objects, with the study area being only about 75 km<sup>2</sup>. The first method can more effectively reflect soil information on different scales within the whole basin. With a comprehensive grid sampling method being used in the basin, comparison is made among sampling points evenly distributing throughout the basin in six scales, which effectively avoids the overgeneralization of results of studies in small and medium scales.

Karst stony desertification is one of the main types of land desertification [21]. It is based on the fragile ecological environment and driven by extremely unreasonable human activities, with the degradation of land productivity as the essence and with the appearance of similar desert landscapes as the symbol [21]. The interference of unreasonable human activities exacerbates the evolution and landscape fragmentation progress of Karst area landscapes characterized by "stony desertification", and thus accurately reflecting the spatial distribution pattern of stony desertification areas plays an important role in the study on stony desertification areas [22]. As for how to describe the spatial variability better, it is of great practical significance to exactly visualize the relations between spatial distribution and sampling scales in stony desertification areas [23]. The spatial distribution characteristics of stony desertification in the Houzhai River Basin are closely related to topography and geomorphology of the watershed, of which, in the east there are mainly peaks and low-lying lands, in the north, south and southwest, there are mountains, and in the middle and west, there are mainly plains and hills, dotted with a few of hills. Corresponding to topographical and geomorphologic features, stony desertification in this watershed is mainly concentrated in the peaks and low-lying lands in the east, the mountainous areas in the north, south and southwest, as well as buttes in the middle and west.

#### *4.2 Influencing Factors of Stony Desertification in Different Sampling Scales*

The results show that with the increase of the study scale, the spatial correlation of rock bareness rate changes from moderate spatial correlation to strong spatial correlation; meanwhile, in studies of large scales, the correlation of gradient, elevation and gradient position with the rock bareness rate is weakened, and rock contents and soil thickness have become the key factors influencing stony desertification in studies of large scales. This conclusion has been widely recognized by other experts, and Wang Dian Jie et al. also believe that different topographic factors act on different scales, and impacts of gradient and elevation are mainly manifested in small and medium studies [24]. With the increase of the study scale, the correlation between rock contents and soil properties is more significant. It is believed by Chen Shengzi et al. that scale variance on large scales increases with fluctuations as the scale is rising, and at this moment, stochastic effects have no obvious influences on soil properties [25].

Gradient and rock bareness rate of Houzhai River Basin are increasing with the rise of elevation, while the soil thickness decreases accordingly. As we all know, at high elevations, geographical and climatic conditions are poor, not suitable for plant growth usually. However, due to lack of arable lands, soil at high elevations of the basin is still used for food production, which, eventually, aggravates the evolution of stony desertification in Karst areas. Through comprehensive analysis, it is found that gradient, rock bareness rate, and soil thickness are the main factors determining the degree of stony desertification [26]. Stony desertification is a serious problem in Houzhai River Basin. Gradient and elevation are important factors leading to soil erosion and stony desertification. The larger the gradient

is, the more serious the soil erosion caused by overland runoff is, thus causing stony desertification. As the elevation increases, the environmental conditions become worse, including increase of gradient and reduction of soil thickness. The vegetation condition becomes worse and worse, with soil and water conservation capacity at high elevations being weak relatively. In addition, in this study, it is also discovered that the key factors influencing the spatial variability of rock bareness rate vary with the sampling scales. On small scales, it is influenced by many factors, on medium scales, it is influenced by gradient, rock contents and rock bareness rate, and on large scales, the soil thickness and rock bareness rate are the key factors influencing the spatial variability of rock bareness rate.

## 5 Conclusions

In this paper, according to the study of the spatial distribution of rock bareness rate and its influencing factors in different sampling scales in small Karst watersheds, there is no big difference in rock bareness rates on different scales, among which the average rock bareness rate is 15.94 % on the scale of 150m × 150m, which is the largest, and the average rock bareness rate is 9.89% on the scale of 900m × 900m, which is the smallest. With the increase of the sampling scale, gradually the maximum value and the average value of rock bareness rate decrease while the coefficient of variability increases. In the scale of 150m × 150m, the areas of minor stony desertification, medium stony desertification and major stony desertification in the Houzhai River Basin are 7.81 km<sup>2</sup>, 4.50 km<sup>2</sup>, and 1.87 km<sup>2</sup>, respectively. The key factors influencing the spatial variability of rock bareness rate vary with sampling scales. On small scales (150m × 150m, 300m × 300m, and 450m × 450m), the spatial variability of rock bareness rate is influenced by gradient, elevation, soil thickness, and rock bareness rate jointly, on medium scales (600m × 600m), it is impacted by gradient, rock content and rock bareness rate, and on large scales (750m × 750m and 900m × 900m), soil thickness and rock bareness rate are the key factors influencing the variability of rock bareness rate.

**Acknowledgments:** This work was financially supported by the National Key Basic Research Development Program (Grant No. 2013CB956702); The first class discipline construction project in Guizhou province (GNYL [2017]007); Regional fund of the National Natural Science Foundation of China [Grant No. 41561075]; and 100 High Level Innovating Project [Grant No. QKHRC-2015-4022].

**Author Contributions:** Zhenming Zhang and Yunchao Zhou carried out the calculation, result analysis and drafted the manuscript, which was revised by all authors. All authors gave their approval of the version submitted for publication.

**Conflicts of Interest:** The authors declare no conflict of interest.

## References

1. Kerry, R.; Oliver, M.A. Average variograms to guide soil sampling. *International Journal of Applied Earth Observation and Geoinformation*. **2004**, *5*, 307-325.
2. Chen, X.B.; Zheng, H.; Zhang, W.; He, X.Y.; Li, L.; Wu, J.S.; Huang, D.Y.; Su, Y.R. Effects of land cover on soil organic carbon stock in a karst landscape with discontinuous soil distribution. *Journal of Mountain Science*. **2014**, *11*, 774-781.
3. Kerry, R.; Oliver M.A. Comparing sampling needs for variograms of soil properties computed by the method of moments and residual maximum likelihood. *Geoderma*, **2007**, *140*, 383-396.
4. Marcos, R.N.; Fabrício P.P.; José A.M.D.; Roney B.O.; Marcelo L.C. and Everson, C. Optimum size in grid soil sampling for variable rate application in site-specific management. *Scientia Agricola*. **2011**, *63*, 386-392.

5. Yu, D.S.; Zhang, Z.Q.; Yang, H.; Shi, X.Z.; Tan, M.Z.; Sun, W.X.; Wang H.J. Effect of soil sampling density on detected spatial variability of soil organic carbon in a red soil region of China. *Pedosphere*. **2011**, 21, 207-213.
6. Webster, R. ; Oliver, MA. Sample adequately to estimate variograms of soil properties. *Journal of Soil Science*. **1992**, 43,177-192.
7. Gascuel-Oudou, C.; Boivin, P. Variability of variograms and spatial estimates due to soil sampling: A case study. *Geoderma*.**1994**, 62, 165-182.
8. Heilman, J.L.; Litvak, M.E.; Mcinnes, J.M.; Kjelgaard, J.F.; Kamps, R.H.; Schwinning S. Water-storage capacity controls energy partitioning and water use in karst 470 ecosystems on the Edwards Plateau,Texas. *Ecohydrology*. **2014**, 7,127-138.
9. Li, Y.B.; Xie, J.; Luo, G.J.; Yang, H.; Wang, S.J. The Evolution of a Karst Rocky Desertification Land Ecosystem and Its Driving Forces in the Houzhaihe Area. *Open Journal of Ecology*. **2015**, 5,501-512.
10. Bach, M.A.; Freibauer, C.; Siebnea, C.; Flessa, H. The German Agricultural Soil Inventory: sampling design for a representative assessment of soil organic carbon stocks. *Procedia Environmental Sciences*. **2011**, 7, 323–328.
11. Liu, Z.T.; Liu C.Q.; Lang, Y.C.; Hu, D. Dissolved organic carbon and its carbon isotope compositions in hill slope soils of the karst area of southwest China: Implications for carbon dynamics in limestone soil. *Geochemical Journal*. **2014**, 48, 277-290.
12. Mao, D.H.; Wang, Z.M.; Li, L.; Miao, Z.H.; Ma, W.H.; Song C.C.; Ren, C.Y.; Jia M.M. Soil organic carbon in the Sanjiang Plain of China: storage, distribution and controlling factors. *Biogeosciences*. **2015**, 12, 1635-1645.
13. Zhang, W.; Chen, H.S.; Wang, K.L.; Su, Y.R.; Zhang, J.G.; Yi, A.J .The heterogeneity of soil nutrients and their influencing factors in peak-clusters depression areas of karst region. *Scientia Agricultura Sinica*. **2006**, 39, 1828–1835.
14. Reuben C.; Navjot S.S.;Menno S.;Peter, K.L.N. Limestone Karsts of Southeast Asia: Imperiled Arks of Biodiversity. *BioScience*. **2006**, 56,733–742.
15. Bergstrom, D.W.; Monreal, C.M.; Millette, J.A.; King, D.J. Spatial Dependence of Soil Enzyme Activities along a Slope. *Soil Sci. Soc. Am. J*. **1998**, 62, 1302–1308.
16. Hu, W.; Schoenau, J.J.; Si, B.C. Representative sampling size for strip sampling and number of required samples for random sampling for soil nutrients in direct seeded fields. *Precision Agriculture* . **2015**,16, 385–404.
17. Cochran, W.G. *Sampling Techniques*. New York:John Wiley and Sons ,Inc, 1997.
18. Lütticken, R.E. Automation and standardisation of site specific soil sampling. *Precision Agriculture*. **2000**, 2, 179–188.
19. Zhang, J.Y.; Dai, M.H.; Wang, L.C., Zeng, C.F.; Su, W.C. The challenge and future of rocky desertification control in karst areas in southwest China. *Solid Earth Discussions*. **2015**, 7, 3271–3292.
20. Zhang, W.; Chen, H.S.; Wang, K.L.; Su, Y.R.; Zhang, J.G.; Yi, A.J. The heterogeneity and its influencing factors of soil nutrients in peak-cluster depression areas of Karst region. *Agricultural Sciences in China*. **2007**. 6, 322–329.
21. Wang, D.J.; Shen, Y.X.; Huang, J. Epilithic organic matter and nutrient contents in three different karst
24. Shen, Y.X.; Liu, W.Y.; Li, Y.H.; Cui, J.W. Community ecology study on karst semi-humid evergreen broad-leaved forest at the central part of Yunnan. *Guihaia*. **2005**, 25, 321–326.
22. Jiang, Z.; Lian, Y.; Qin, X. Rocky desertification in Southwest China: Impacts, causes, and restoration. *Earth-Science Reviews*. **2014**, 132, 1–12.
23. Liu, C.Q. Biogeochemical processes and cycling of nutrients in the earth's surface: Cycling of nutrients in soil-plant plant systems of karstic environment, Southwest China. Beijing: Science Press. **2009**;80-96.
24. Wang, D.J.; Shen, Y.X.; Huang, J.; Li, Y.H. Rock outcrops redistribute water to nearby soil patches in karst

landscapes. *Environ Sci Pollut Res.* **2016**, 23, 8610–8616.

25. Chen, S.Z.; Zhou Z.F.; Yan L.H.; Li B. Quantitative Evaluation of Ecosystem Health in a Karst Area of South China. *Sustainability.* **2016**, 8, 975-989.

26. Li, C.; Xiong, K.N.; Wu, G.M. Process of biodiversity research of karst areas in China. *Acta EcologicaSinica.* **2013**, 33: 192–200.